COMPARATIVE STUDY OF THE AERODYNAMIC PERFORMANCES OF MOTORCYCLE RACING WHEELS USING NUMERICAL CFD SIMULATIONS

F. CONCLI[1], M. GOBBI[2] & C. GORLA[2]

[1]Free University of Bolzano/Bozen, Faculty of Science and Technology, Bolzano, Italy
[2]Politecnico di Milano, Department of Mechanical Engineering, Milano, Italy

ABSTRACT

In motorcycle competitions, aerodynamics plays a fundamental role. In order to improve the performance of racing motorbikes, different front-wheel geometries have been studied by means of numerical CFD simulations. Different lean angles were analysed for each geometry and the air motion-field were calculated. The considered geometries range from standard spoked design to solid wheels. Both steady-state and dynamic simulations were run using the open-source free software OpenFOAM®. This open-source code was selected because, like all the computer programs of this type, it allows a higher flexibility with respect to any close-source commercial software, allowing a customization of the code by implementing specific models for the analysis of the physical problem of interest and also, at the same time, a higher parallelization of the computations.

Steady-state simulations were performed using a rotating reference frame (MRF) while, for the transients, a partially-rotating mesh was adopted, thus taking advantage of the internal sliding interfaces (AMI).

Drag, lift and force-moments have been calculated with the aim of examining the stability and manoeuvrability of the different configurations.

1 INTRODUCTION

Differently from every-day applications [1], in car and motorcycle competitions, aerodynamics is fundamental and the racing teams are becoming increasingly aware of it: minimal time differences on each lap can affect the race results. The high costs of wind-tunnel tests act still as a deterrent to an experimental-driven aerodynamic design of vehicles, but in the last years CFD modelling gives an important contribution in bypassing this problem and to widespread a more aware use of some design solutions.

Concerning in particular the motorcycles, the main contributors to aerodynamic forces in such a vehicle are well-know and are: the rider, the bodywork and the wheels. Burke [2] and Lukes et al [3] tried to identify the most relevant contributions to the overall aerodynamic resistance. Greenwell et al [4] have observed that the average contribution of the wheels to the total drag is approximately 10-15% and that relevant improvements are still possible. For example, Zdravkovich [5] showed that the adoption of proper flaps could lead to a drag reduction up to 5%. Tew and Sayers [6] have compared the aerodynamic performance of optimized and traditional wheels. They observed a reduction of the drag up to 50%.Kyle and Burke [7 - 9] observed a significant drag reduction for rotating wheels with respect to stationary ones. The same trend was observed by Fackrell and Harvey [10 - 12] for car tires.

Few examples of CFD applied to study the air flow around a rotating wheel in contact with the ground can be found in the actual scientific literature. Wray [13] performed numerical simulations to investigate the effect of the yaw angle on the drag and lift forces. McManus et al [14] use the results proposed by Fackrell and Harvey to validate their CFD results. Godo et al [15] observed a transition from the expected downforce to a lift force at a yaw angle between 5 and 8 degrees. A comprehensive study of the flows around bike wheels and the related forces was made by Godo el at [16].

In this paper, the authors applied an open-source CFD simulation code, OpenFOAM® [17] to study the aerodynamic forces acting on a racing motorbike wheel in different operating conditions. Both steady state and dynamic simulations were performed   at different lean angles and with three wheel profiles. More in detail, steady state simulations were performed adopting a rotating reference frame (MRF) [18] coupled with a solver specifically thought for incompressible flows. Transient simulations were performed by partitioning properly the spatial computational domain, by setting as rotating a part of the mesh and adopting arbitrary interfaces (AMI) [19].

2 WHEEL GEOMETRY AND OPERATING CONDITIONS

Different front wheel geometries have been analysed. The reference geometry (namely: "REF7") has 7 spokes. The second wheel ("MGD6") has 6 spokes, while the last one is a solid-disk wheel ("DSKW"). All the three wheels mount the same tire.
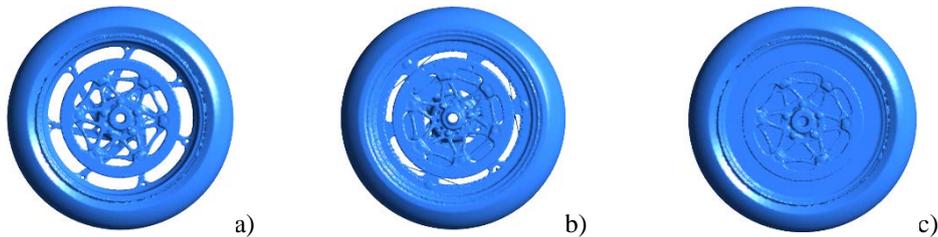

a)   b)   c)

Figure 1: Analysed wheel geometries; a) REF7; b) MGD6; c) DSKW.

3 MODEL SET-UP

Each of the presented wheels was modelled as if it was in contact with the ground, for a greater similarity with reality. The dimensions of the computational domain have been chosen to be sufficiently large to not influence the results (i.e., including a fully-developed aerodynamic wake) however letting the solver converge in a reasonable amount of time.

A cylindrical partition of the domain, containing the wheel rim only (i.e. not the tire), allows to apply a rotating reference frame or to set into rotation the wheel boundary.

Both on the "Ground" and on "Wheel" and "Tire", three prismatic boundary layers have been created. The height of the first cell was selected in order to maintain the y+ value between 50 and 500. In this manner, the velocity profile can be correctly reconstructed by applying wall functions.
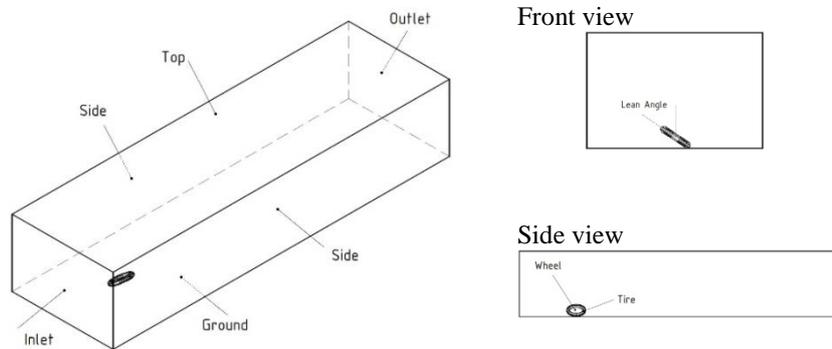

Figure 2: Mesh partitioning and boundaries.

Table 1: Boundary conditions.

	Ground	Sides/Top	Inlet	Outlet	Wheel	Tire
					MRF/AMI	MRF/AMI
U	fixedValue unif. 60 m/s	symmetry	fixedValue unif. 60 m/s	zeroGradient	movingWallVelocity unif. 0 m/s	movingWallVelocity unif. 0 m/s
p	zeroGradient	symmetry	zeroGradient	fixedValue unif.1E5Pa	zeroGradient	zeroGradient
eps	epsilonWallFunction	symmetry	fixedValue	inletOutlet	epsilonWallFunction	epsilonWallFunction
k	kqRWallFunction	symmetry	fixedValue	inletOutlet	kqRWallFunction	kqRWallFunction

A uniform velocity profile was applied both to the "Inlet" and to the "Ground" surfaces, in order to simulate a constant travelling speed of the motorbike. The pressure at the "Outlet" surface was set to 1 bar (ambient absolute pressure). The surfaces of the "Wheel" and the "Tire" were treated as moving walls. Their velocities are referred to the rotating reference frame (rotating frame – steady simulations, or rotating mesh – transient simulations). For this reason, the relative velocity has been set to zero. The rotational

velocity of the wheel and of the tire was set to 0.05 rad/s. For a tire radius of 0.299 m, this leads to a tangential velocity of 60 m/s.

3.1 MRF approach – steady state calculations

The MRF model is a steady-state approximation in which individual cell zones move at different rotational speeds [20]. The flow at each moving cell zone is solved using the equations in the moving reference frame , including also the additional terms related to the Coriolis acceleration ($2\boldsymbol{\omega} \times \boldsymbol{v_r}$) and the centripetal acceleration ($\boldsymbol{\omega} \times \boldsymbol{\omega} \times \boldsymbol{r}$) into the momentum conservation equation:

$$\frac{\partial}{\partial t}(\rho\boldsymbol{v_r}) + \nabla \cdot (\rho\boldsymbol{v_r}\boldsymbol{v_r}) + \rho(2\boldsymbol{\omega} \times \boldsymbol{v_r} + \boldsymbol{\omega} \times \boldsymbol{\omega} \times \boldsymbol{r}) = -\nabla p + \nabla \cdot [\mu(\nabla\boldsymbol{v_r} + \nabla\boldsymbol{v_r^T})] + \rho\boldsymbol{g} + \boldsymbol{F} \text{ (1)}$$

where: p is the pressure, ρ is the density, μ is the viscosity, $\boldsymbol{g}$ is the gravitational force, $\boldsymbol{F}$ represents the resultant of the external body forces, $\boldsymbol{\omega}$ is the angular velocity referred to a stationary (inertial) reference frame and $\boldsymbol{v_r} = \boldsymbol{v} - \boldsymbol{\omega} \times \boldsymbol{r}$, where $\boldsymbol{r}$ is the position vector from the origin of the rotating frame.

The continuity equation is written in terms of relative velocities:

$$\frac{\partial \rho}{\partial t} + \nabla \cdot (\rho\boldsymbol{v_r}) = 0 \qquad\qquad (2)$$

At the interfaces between the two cell zones, a local reference frame transformation is performed to enable flow variables in one zone to be used to calculate fluxes at the boundary of the adjacent zone. It should be noted that the MRF approach does not account for any relative motion of a moving zone with respect to its adjacent zones; the grid remains fixed for the computation. This is analogous to freezing somehow the motion of the moving part in a specific position and observing the instantaneous flow-field with the rotor in that position. Although the MRF approach is clearly an approximation, it can provide a reasonable modelling of the flow for many applications, by considerably reducing the computational effort with respect to the sliding mesh approach. However, the MRF model does not accurately simulate the transient start-up but gives just a regime solution of an unsteady problem.

3.2 AMI approach – transient calculations

The approach, in which a portion of the grid is set into rotation (here referred to as AMI), is able to correctly describe the transient start-up but it is more computationally demanding with respect to the MRF approach [20].

The common surface of adjacent cell zones (partitions) forms an arbitrary mesh interface (AMI). In this specific case, the interface is a cylindrical surface. The internal cell zone will slide along the mesh interface in discrete steps. The AMI operates by projecting the patches of the boundary mesh of one partition onto the other. This ensures that the values of a generic field are the same on both sides of the interface.

3.3 Other techniques

Another option is to have one single partition, and to move the boundaries corresponding to wheel and tire but this will lead to a mesh distortion. When the quality of the computational grid decreases under a set level, it should be updated [21]. This approach

is very powerful but also computationally demanding. A reduction of the calculation effort can be achieved by updating only part of the grid (taking advantage of partitioning as in MRF and ADI) [22] or by using advanced mesh-handling algorithms [23-24].

4 NUMERICAL SETTINGS

For compressible flows, the unknown quantities are the velocity components and the density, while the pressure is evaluated by using the constitutive equation. For incompressible flows, however, the variables are the pressure and the velocity components. Such a system of equations for incompressible flows has a solution because there are no equations where the pressure is explicitly defined. To calculate it, the continuity equation is substituted with a pressure equation; after some manipulation of the formulae, the pressure appears as the unknown term in the momentum equation.

For steady-state calculations, the SIMPLE (Semi Implicit Method for Pressure- Linked Equations) scheme was adopted to solve the pressure-velocity-coupling, while for transient analyses, a PIMPLE (merged PISO-SIMPLE) scheme was adopted.

The SIMPLE algorithm was developed with the aim of reaching a very fast convergence. This approach is very effective but does not contain any time-domain information. To provide a numerically-stable simulation, a relaxation factor is usually introduced. The PISO algorithm, developed for transient simulations, is time-conservative. The drawback is that, to ensure the convergence, the time step should be reduced significantly and, consequently, the simulation time increases. The PIMPLE combines both methods, performing all iterations in SIMPLE mode (with relaxation) to ensure convergence also for large time steps and performing also an additional final iteration without relaxation in PISO mode to ensure the time consistency.
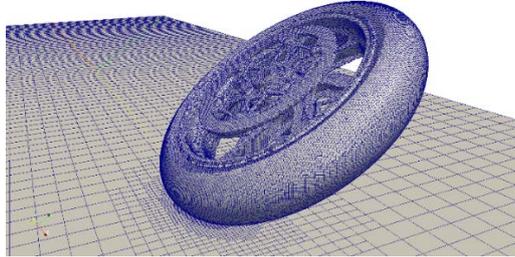

Figure 3: Details of the mesh for the wheel and the ground in the contact point.

5 RESULTS

Forces on each wheel geometry are reported (table 2) into the separate components corresponding to: the drag force (// to the motorbike velocity), the lift force ($\perp$ to the axis of the wheel and to the velocity of the motorbike) and the lateral force (// to the wheel axis) [25]. The shear between inertial and viscous contributions is also shown.

Figure 4 and 5 show the velocity contour plot on the axial symmetry plane of the wheel and the vorticity. Vorticity is defined as:

$$\varpi = \nabla \times u \tag{3}$$

where u is the velocity vector. Vorticity describes the local spinning motion of the fluid. It has been observed that an increase in the vorticity is related to a reduction of the drag forces. This is because a shifting downstream of the flow separation point corresponds to a higher vorticity [26].
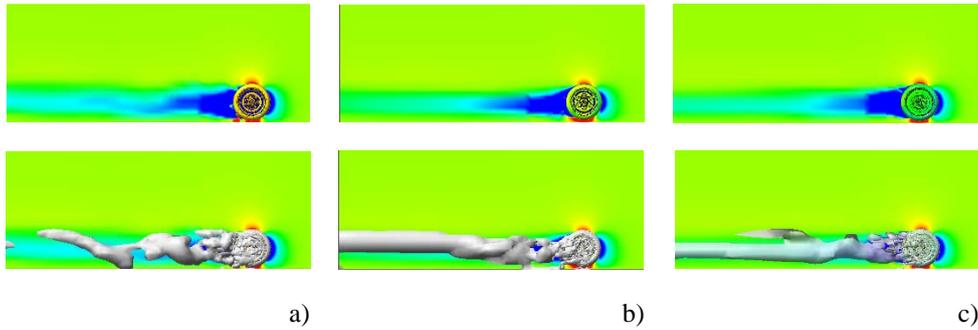

a)   b)   c)

Figure 4: velocity contour plot and vorticity – wheel mid plane: a) REF7; b) MGD6; c) DSKW

a)   b)   c)
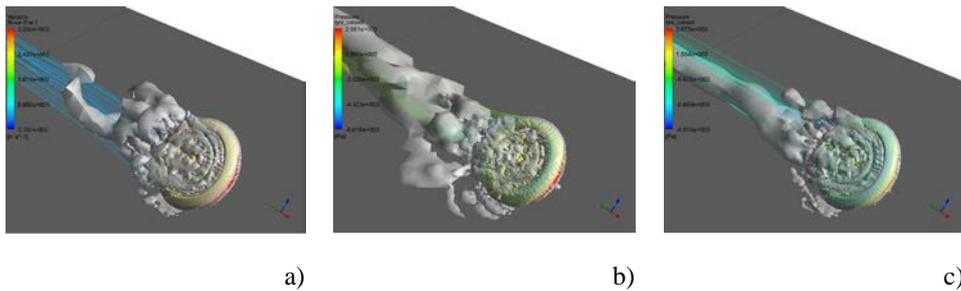
Figure 5: velocity contour plot and vorticity: a) REF7; b) MGD6; c) DSKW

Table 2: Drag and lift – steady state calculations.

	Total (inertial, viscous) forces		
	REF7	**MGD6**	**DSKW**
Drag [N] (y)	163.16 (156.96, 6.20)	93.32 (87.57, 5.75)	72.15 (66.18 5.97)
Lift [N] (x)	-14.48 (-14.95, 0.47)	-24.26 (-24.63, 0.47)	-27.89 (-28.59 0.69)
Axial [N] (z)	-51.52 (-51.43 -0.08)	-73.64 (-73.46 -0.18)	-15.62 (-15.52 -0.10)

A significant reduction of the drag can be observed with the new MGD6 geometry with respect to the reference one (REF7). DSKW ensures a further reduction. On the other side, the lift force increases (from REF7 to DSKW). Instead, the axial force has an oscillating trend.

Inertial effects control the drag, the lift and the axial forces. Viscous effects are comparable for the different geometries, but their contribution is of a lower order of magnitude.

The frontal surface area is equal to 0.09 m^2 (for each design). The corresponding drag coefficients result to be: 0.55 (REF7), 0.40 (MGD6) and 0.35 (DSKW).

6 CONCLUSIONS

Different racing motorbike wheel geometries were studied in terms of drag, lift and axial forces with a CFD approach. The results of the simulations have shown that the drag force can be halved by introducing a solid disk design. However, the wider lateral surface of this design is associated with additional axial forces that may reduce the drivability and manoeuvrability of the motorbike.

The considered different solutions show both benefits and limitations that deserve to be inquired further, so a second and more detailed study will follow this initial screening.

REFERENCES

[1] Bietresato, M, Friso, D, Sartori, L., 2012, "Assessment of the efficiency of tractor transmissions using acceleration tests", Biosyst. Eng., 112, pp. 171-180.
[2] Kyle, C.R, "Selecting Cycling Equipment", 2003. In High Tech Cycling, 2nd Edition, Burke, E.R, ed. Human Kinetics, pp. 1-48.
[3] Lukes, R.A., Chin, S.B. and Haake, S.J., "The Understanding and development of Cycling Aerodynamics", 2005, Sports, Engineering, 8, pp. 59-74.
[4] Greenwell, D.I., Wood, N.J., Bridge, E.K.L and Add, R.J. 1995, "Aerodynamic characteristics of low-drag bicycle wheels", Aeronautical J., 99 (983), pp. 109-120.
[5] Zdravkovich, M.M., 1992, "Aerodynamics of bicycle wheel and frame", J. Wind Engg and Indust. Aerodynamics, 40, pp. 55-70.
[6] Tew, G.S. and Sayers, A.T., 1999, "Aerodynamics of yawed racing cycle wheels", J. Wind Eng. Industr. Aerodynamics, 82, pp. 209-222.
[7] Kyle, C.R. and Burke, E. 1984, "Improving the racing bicycle", Mech. Eng., 106, pp. 34-35.
[8] Kyle, C.R., 1985, "Aerodynamic wheels", Bicycling, pp. 121-124.
[9] Kyle, C.R., 1991, "New aero wheel tests", Cycling Sci. pp. 27-32
[10] Fackrell, J.E. and Harvey, J.K., 1973, "The Flowfield and Pressure Distribution of an Isolated Road Wheel", Advances on Road Vehicle Aerodynamics", Stephens, H.S., ed., BHRA Fluid Engineering, pp. 155-165.
[11] Fackrell, J.E., 1974, "The Aerodynamics of an Isolated Wheel Rotating in Contact with the Ground", Ph.D. Thesis, University of London, London, U.K.
[12] Fackrell, J.E. and Harvey, J.K., 1975, "The Aerodynamics of an Isolated Road Wheel", in Pershing, B. ed., Proc. of 2nd AIAA Symposium of Aerodynamics of Sports and Competition Automobiles, LA, Calif., USA, pp. 119-125.
[13] Wray, J, 2003, "A CFD Analysis into the effect of Yaw Angle on the Flow around an Isolated Rotating Wheel", Ph.D. Thesis, Cranfield University, U.K.
[14] McManus, J. and Zhang, X., 2006, "A Computational Study of the Flow Around an Isolated Wheel in Contact with the Ground", J. Fluids Engineering, 128, pp. 520-530.

[15] Godo, M.N, Corson, D. and Legensky, S.M., 2009, "An Aerodynamic Study of Bicycle Wheel Performance using CFD", 47th AIAA Aerospace Sciences Annual Meeting, Orlando, FL, USA, 5-8 January, AIAA Paper No. 2009-0322.

[16] Godo, M.N, Corson, D. and Legensky, S.M., 2010, "A comparative Aerodynamic study of commercial bicycle wheels using CFD", 48th AIAA Aerospace Sciences Annual Meeting, Orlando, FL, USA, 4-7 January, AIAA Paper No. 2010-1431.

[17] OpenFOAM®, www.openfoam.com

[18] Concli, F., Gorla, C., 2016, "Windage, churning and pocketing power losses of gears: different modeling approaches for different goals", Forschung im Ingenieurwesen/Engineering Research, 80 (3-4), pp. 85-99.

[19] Concli, F., Gorla, C., 2017, "Numerical modeling of the churning power losses in planetary gearboxes: An innovative partitioning-based meshing methodology for the application of a computational effort reduction strategy to complex gearbox configurations", Lubrication Science, 29 (7), pp. 455-474.

[20] Concli, F., Gorla, C., Della Torre, A., Montenegro, G., 2015, "Churning power losses of ordinary gears: A new approach based on the internal fluid dynamics simulations", Lubrication Science, 27 (5), pp. 313-326.

[21] Concli, F., Gorla, C., 2012, "Analysis of the oil squeezing power losses of a spur gear pair by mean of CFD simulations", ASME 2012 11th Biennial Conference on Engineering Systems Design and Analysis, ESDA 2012 (2), pp. 177-184.

[22] Concli, F., Gorla, C., Stahl, K., Höhn, B.-R., Michaelis, K., Schultheiß, H., Stemplinger, J.-P., 2013, "Load independent power losses of ordinary gears: Numerical and experimental analysis", 5th World Tribology Congress, WTC 2013, 2, pp. 1243-1246.

[23] Concli, F., Della Torre, A., Gorla, C., Montenegro, G., 2016, "A New Integrated Approach for the Prediction of the Load Independent Power Losses of Gears: Development of a Mesh-Handling Algorithm to Reduce the CFD Simulation Time", Advances in Tribology, 2016, art. no. 2957151

[24] Concli, F., Gorla, C., 2016, "Numerical modeling of the power losses in geared transmissions: Windage, churning and cavitation simulations with a new integrated approach that drastically reduces the computational effort", Tribology International, 103, pp. 58-68.

[25] Concli, F., 2016, "Thermal and efficiency characterization of a low-backlash planetary gearbox: An integrated numerical-analytical prediction model and its experimental validation", Proceedings of the Institution of Mechanical Engineers, Part J: Journal of Engineering Tribology, 230 (8), pp. 996-1005.

[26] Rasedul Islam, Md., et al, 2013, "Drag Reduction of a Car by Using Vortex Generator", International Journal of Scientific & Engineering Research, 4 (7), pp. 1298-1302